Published in final edited form as:
Neuroscience. 2012 November 8; 224C: 63–69. doi:10.1016/j.neuroscience.2012.08.017.

Expression of $Ca_V3.2$ T-Type Ca^{2+} Channels in a Subpopulation of Retinal Type-3 Cone Bipolar Cells

Jinjuan Cui, **Elena Ivanova**, **Lu Qi**, and **Zhuo-Hua Pan**
Department of Ophthalmology and Anatomy/Cell Biology, Wayne State University School of Medicine, Detroit, MI

Abstract

Retinal bipolar cells and ganglion cells are known to possess voltage-gated T-type Ca^{2+} channels. Previous electrophysiological recording studies suggested that there is differential expression of different T-type Ca^{2+} channel α1 subunits among bipolar cells. The detailed expression patterns of the individual T-type Ca^{2+} channel subunits in the retina, however, remain unknown. In this study, we examined the expression of the $Ca_V3.2$ Ca^{2+} channel α1 subunit in the mouse retina using immunohistochemical analysis and patch-clamp recordings together with a $Ca_V3.2$ knock out (KO) mouse line. The specificity of a $Ca_V3.2$ Ca^{2+} channel antibody was first confirmed in recombinant T-type Ca^{2+} channels expressed in HEK (human embryonic kidney) cells and in $Ca_V3.2$ KO mice. Our immunohistochemical analysis indicates that the $Ca_V3.2$ antibody labels a subgroup of type-3 cone bipolar cells (CBCs), the PKAβII-immunopositive type-3 CBCs. The labeling was observed throughout the cell including dendrites and axon terminals. Our patch-clamp recording results further demonstrate that $Ca_V3.2$ Ca^{2+} channels contribute to the T-type Ca^{2+} current in a subpopulation of type-3 CBCs. The findings of this study provide new insights into understanding the functional roles of T-type Ca^{2+} channels in retinal processing.

Keywords

T-type Ca^{2+} current; $Ca_V3.2$ Ca^{2+} channel α1 subunit; type 3 bipolar cell; retina; knockout mouse; immunostaining

Introduction

T-type Ca^{2+} channels play a variety of roles in the central nervous system, including controlling membrane excitability, pacemaker activity, intracellular Ca^{2+} concentration, and hormone secretion (Huguenard, 1996; Perez-Reyes, 2003; Carbone et al., 2006). Three isoforms of poreforming T-type Ca^{2+} channel α1 subunits, $Ca_V3.1(\alpha1_G)$, $Ca_V3.2(\alpha1_H)$, and $Ca_V3.3(\alpha1_I)$, have been cloned and characterized (Perez-Reyes, 2003; 2006). T-type Ca^{2+} currents with different α1 subunits exhibit distinct biophysical properties (McRory et al., 2001). T-type Ca^{2+} channels are also subject to subunit-specific modulations (Todorovic et al., 2001; Chemin et al., 2006; Traboulsie et al., 2007; Hildebrand et al., 2007; Nelson et al.,

Address correspondence to-- Zhuo-Hua Pan, Ph.D. Department of Ophthalmology and Anatomy & Cell Biology Wayne State University School of Medicine 540 E. Canfield Avenue Detroit, MI 48201 Tel. 313-577-9830; fax 313-577-3125 zhpan@med.wayne.edu.

2007; Perez-Reyes, 2010). Heterogeneous expression of different isoforms of T-type Ca^{2+} channels has been reported in the CNS (Talley et al., 1999) and contributes to distinct neuronal physiological functions (Chemin et al., 2002; Molineux et al., 2006; Cain and Snutch, 2010).

T-type Ca^{2+} currents have been well documented in mammalian retinal neurons, including retinal bipolar cells (Kaneko et al., 1989; Protti & Llano, 1998; Pan, 2000) and ganglion cells (Sherwin et al., 2003). Previous studies reported the evidence of a differential expression of different isoforms of T-type Ca^{2+} channel α1 subunits among retinal bipolar cells (Hu et al., 2009). The expression patterns of the individual T-type Ca^{2+} channel subunits in the retina, however, remain unknown. In this study, using immunohistochemical analysis and electrophysiological recordings together with $Ca_v3.2$ knockout (KO) mice, we investigated the expression of $Ca_v3.2$ T-type Ca^{2+} channels in the mammalian retina. We found that $Ca_v3.2$ Ca^{2+} channels are expressed in a subtype of retinal cone bipolar cells (CBCs).

Methods:

HEK cell culture and DNA transfection

HEK-293 cells were maintained in Dulbecco's modified Eagle's medium (Gibco/BRL, Grand Island, NY) supplemented with 10% fetal bovine serum, 100 U/ml penicillin G, and 100 μg/ml streptomycin at 37°C in a humidified atmosphere of 95% air and 5% CO_2. For DNA transfection experiments, the cells were seeded in 35-mm dishes and transfected with cDNAs for rat Cav3.1, human Cav3.2, or rat Cav3.3 (kindly provided by Dr. Perez-Reyes) using Lipofectamine (Invitrogen, San Diego, CA). Immmunostaining was performed ~24 h after the transfection.

Animals

C57BL/6J mice were purchased from Jackson Laboratory (Bar Harbor, ME). A $Ca_v3.2$ KO mouse line, B6.129-*Cacna1h*^{tm1Kcam}, which developed in the Campbell laboratory at the University of Iowa (Chen et al., 2003), was obtained from the Mutant Mouse Regional Research Center (#009979-MU). The $Ca_v3.2$ KO mice were generated on a mixed C57BL/6J and 129 background and backcrossed to C57BL/6J mice for at least 6 generations. Mice were genotyped by PCR using the following primers: wild type forward primer, 5'- ATT CAA GGG CTT CCA CAG GGT A-3', mutant forward primer, 5'-GCT AAA GCG CAT GCT CCA GAC TG-3'; common reverse primer 5'-CAT CTC AGG GCC TCT GGA CCA C-3'. The PCR conditions were 94°C for 3 min, followed by 35 cycles of 94°C for 45 sec, 66°C for 45 sec, 72°C for 45 sec, and 72°C for 10 min. The PCR product sizes were as follows: mutant = 330 bp; heterozygote = 330 bp and 480 bp; wild type = 480 bp. All animal-handling procedures were approved by the Institutional Animal Care and Use Committee at Wayne State University and were in accordance with the NIH Guide for the Care and Use of Laboratory Animals.

Immunohistochemistry

Mice at 1–2 months of age were deeply anesthetized with CO_2 and decapitated. The retinas in the eyecup were fixed in 4% paraformaldehyde in 0.1 M phosphate buffer (PB) for 20 minutes. The isolated retinas were successively cryoprotected in a gradient of varying sucrose concentrations (10%, 20%, and 30% w/v in PB), and vertical sections (20 μm thick) were cut with a cryostat.

Retinal sections were blocked for 1 hour in PB containing 5% Chemiblocker (membrane-blocking agent; Chemicon), 0.5% Triton X-100 and 0.05% sodium azide (Sigma). The

primary antibodies were goat polyclonal anti-T-type Ca^{2+} $Ca_v3.2$ (1:100; Cat # sc-16263; Santa Cruz), mouse anti-protein kinase A regulatory subunit IIβ (PKAIIβ, 1:80000; Cat # 610625; BD), rabbit anti-hyperpolarization-activated and cyclic nucleotide-gated channel 4 (HCN4, 1:500, Cat # APC-052, Alomone), rabbit anti-recoverin (1:2000; Cat # AB5585; Chemicon), mouse anti-calsenilin (1:2000; kindly provided by Dr. Wasco, Harvard Medical School), and mouse anti-calretinin (1:10000; Cat # MAB1568; Chemicon). The primary antibodies were diluted in the same PB solution and applied overnight, followed by incubation (1–2 h) in the secondary antibodies that were conjugated to Alexa 555 or Alexa 594 (1:600; red fluorescence; Invitrogen) or Alexa 488 (1:600; green fluorescence; Invitrogen). All steps were performed at room temperature.

All images were acquired using a Zeiss Axioplan 2 microscope with an Apotome oscillating grating to reduce out-of-focus stray light. Image projections were constructed by collapsing individual z-stacks of optical sections onto a single plane. The brightness and the contrast were adjusted using Adobe Photoshop.

Patch-clamp recordings

Retinal slices were prepared according to previously described procedures (Cui et al., 2003). The recording chamber was continuously superfused with bubbled Ames solution at a rate of ~2 ml/min. The electrode solution contained (in mM): CsCl 120, TEA-Cl 20, $MgCl_2$ 1, $CaCl_2$ 0.5, EGTA 5, HEPES 10, Na-GTP 0.5 and Mg-ATP 6; pH 7.3. The fluorescent dye Alexa 568 was added to the electrode solution at a concentration of 100 μM. The extracellular solution contained (in mM) 95 NaCl, 5 KCl, 10 $CaCl_2$, 10 CsCl, 20 TEA-Cl, 1 $MgCl_2$, 10 HEPES, and 22.2 glucose, with phenol red, 0.001% v/v, pH 7.2. In all recordings, 100 μM bicuculline, 100 μM TPMPA, 2 μM strychnine, and 1 μM tetrodotoxin (TTX) were included in the extracellular solutions. After the recordings, the retinal slices were fixed with 4% paraformaldehyde for 30 min, followed by blocking for 2 hrs in a solution containing 5% Chemiblocker. The slices were incubated with the primary antibody anti-calretinin at a dilution of 1:5000 for 3–4 days at 4°C. After washing with PB, the slices were treated with a secondary antibody (Donkey anti-mouse Alexa 488) at a dilution of 1:500 for 1 hr in the dark at RT. Specimens were viewed using a Zeiss Axiophot microscope.

Results:

The expression of $Ca_v3.2$ T-type Ca^{2+} channels in the retina was investigated by immunostaining. The specificity of the $Ca_v3.2$ Ca^{2+} channel antibody (Santa Cruz; Cat. 16263) was first examined against recombinant $Ca_v3.2$ T-type Ca^{2+} channels expressed in HEK cells. As shown in Figure 1, immunoreactivity of the $Ca_v3.2$ antibody was observed in HEK cells that were transfected with the $Ca_v3.2$ subunit (Fig. 1A) but not in those that were either untransfected (Fig. 1B) or transfected with $Ca_v3.1$ or $Ca_v3.3$ subunits (data not shown), indicating that the $Ca_v3.2$ antibody is specific for $Ca_v3.2$ channels. In retinal vertical sections, the $Ca_v3.2$ Ca^{2+} channel antibody was found to label a population of cells with their somata located in the inner nuclear layer (Fig. 2A). No staining was observed in retinal sections from $Ca_v3.2$ KO mice (Fig. 2B). The latter finding further confirmed the specificity of the $Ca_v3.2$ antibody in the mouse retina.

Based on their morphological properties, the $Ca_v3.2$-immunopositive cells were found to be bipolar cells because they exhibited dendrites located in the outer plexiform layer (OPL) and axon terminals that narrowly stratified in the inner plexiform layer (IPL) (Fig. 2A). To visualize the axon terminal stratification of the $Ca_v3.2$-immunopositive cells in the IPL, we performed double-labeling for $Ca_v3.2$ and calretinin, a commonly used marker for the stratification of the IPL (Haverkamp and Wässle, 2000). As shown in Figure 2C, the axon

terminals of the $Ca_v3.2$-immunopositive cells were located between the two distal calretinin bands, which are known to define the stratum 2 of the IPL. In the rodent, only type-3 CBCs have their axon terminals stratified in the stratum 2 of the IPL (Euler and Wässle, 1995; Ghosh et al., 2004; Pignatelli and Strettoi, 2004). These results suggest that the $Ca_v3.2$-immunopositive cells are type-3 or a subpopulation of type-3 CBCs.

Two subtypes of type-3 CBCs, termed type-3a and type-3b, have been reported, which can be labeled by antibodies against HCN4 and PKAIIβ, respectively (Mataruga et al., 2007). To confirm that the $Ca_v3.2$-immunopositive cells are in fact type 3 CBCs and also to determine whether they could be subtype of type-3 CBCs, we performed double- labeling of $Ca_v3.2$ with HCN4 or PKAIIβ. As shown in Figures 3A–D, the $Ca_v3.2$-positive cells did not show colabeling with HCN4 as indicated by the lack of overlap staining both in the somata (Fig. 3C) and the axon terminals (Fig. 3D). However, the $Ca_v3.2$-positive cells showed colabeling with PKAIIβ (Fig. 3E–H), as demonstrated by the overlap of $Ca_v3.2$ and PKAIIβ staining in the somata (Fig. 3G) and the axon terminals (Fig. 3H). In addition, the $Ca_v3.2$-positive cells were colabeled neither with recoverin (Fig. 3I–L) nor calsenilin (Fig. 3M–Q), the markers for type-2 CBCs and type-4 CBCs, respectively. The latter finding ruled out the possibility of these cells being type-2 or type-4 CBCs. Taken together, our results indicate the expression of $Ca_v3.2$ Ca^{2+} channels in a subtype of type 3 CBCs – the PKAIIβ-positive type-3 or type-3b CBCs.

We next determined whether $Ca_v3.2$ Ca^{2+} channels contribute to the T-type Ca^{2+} current in type-3 CBCs. For this purpose, whole-cell patch-clamp recordings were performed to record Ca^{2+} currents from type-3 CBCs in retinal slices. Type 3 CBCs were identified based on their axon terminal stratification in stratum 2 of the IPL with dye filling through the recording electrode following by immunolabeling for calretinin (Fig. 4A and B). We first examined the properties of T-type Ca^{2+} current in type-3 CBCs in wild-type animals (C57BL/6J mice). Because bipolar cells are known to possess both T- and L-type Ca^{2+} currents (de la Villa et al., 1998; Pan, 2000), to separate the T-type Ca^{2+} current from the L-type, the Ca^{2+} currents elicited at each test potential (ranging from −60 mV to +10 mV) were depolarized from two different pre-pulses (1 sec) at −80 mV and −50 mV (see left panel in Fig. 4C). The currents evoked from −50 mV should be the L-type Ca^{2+} current, while those evoked from −80 mV should represent a mixture of T- and L-type (the total currents). Therefore, the subtraction of the L-type current from the total current was used to estimate the T-type current (right panel in Fig. 4C). Figure 4D shows the I–V relationship for the total current (black), L-type (blue), and the estimated T-type (red). The T-type Ca^{2+} current was activated at a potential >−60 mV and reached its peak around −30 mV, while the L-type Ca^{2+} current was activated at a potential of >−40 mV and reached to its peak around −30 to −20 mV. It should note that, due to the different activation kinetics of these two currents, the sum of the T-type and L-type currents is greater than the total current for the step to >−40 mV.

Because the L-type Ca^{2+} current was not activated at a potential of −40 mV under our recording conditions, the T-type Ca^{2+} currents evoked by the test pulse to −40 mV from the holding potential of −80 mV in type-3 CBCs were compared in wild-type and $Ca_v3.2$ KO mice to determine the contribution of $Ca_v3.2$ Ca^{2+} channels to the T-type Ca^{2+} current. Because the two types of type-3 CBCs were unable to be distinguished morphologically, the recordings were made from all morphologically identified type-3 CBCs. Figure 5A shows the distribution plot of the current amplitude for the recorded type-3 CBCs in control (n = 29) and $Ca_v3.2$ KO (n = 25) mice. As shown in the Figure 5A, a portion of the recorded type-3 CBCs in $Ca_v3.2$ KO mice exhibited a marked decrease in the T-type Ca^{2+} current. The average of the T-type Ca^{2+} currents from all recorded type-3 CBCs in wild-type and

$Ca_v3.2$ KO mice was 89.9 ± 28.2 (mean ± SD; n = 25) and 59.1 ± 34.5 (n = 29), respectively (Fig. 5B). These two values are significantly different ($P<0.005$).

Discussion:

In this study, we investigated the expression of $Ca_v3.2$ Ca^{2+} channels in the mouse retina. We first validated the specificity of a $Ca_v3.2$ Ca^{2+} channel antibody in the HEK cell expression system and a $Ca_v3.2$ KO mouse line. Our immunostaining results showed that the $Ca_v3.2$ antibody labeled a population of bipolar cells with their axon terminals narrowly stratified in stratum 2 of the IPL, suggesting that they are type-3 CBCs according to the common classification scheme of bipolar cells in the rodent retina. Our detailed immunohistochemistry analysis with bipolar cell markers indicated that $Ca_v3.2$-immunopositive bipolar cells belong to a subtype of type-3 CBCs, the PKAβII-immunopositive type-3 or termed type-3b CBCs (Mataruga et al., 2007). Using whole-cell patch-clamp recordings and comparing the currents between wild-type and $Ca_v3.2$ KO mice, we provided evidence that $Ca_v3.2$ Ca^{2+} channels contribute to the T-type Ca^{2+} current in a subpopulation of type-3 CBCs. Taken together, our studies revealed for the first time the expression pattern of the $Ca_v3.2$ Ca^{2+} channel in the mouse retina.

Our immunostaining results show that labeling of $Ca_v3.2$ is observed throughout the $Ca_v3.2$-postive cell, indicating that the T-type Ca^{2+} channels are localized in the soma, dendrites, and axon terminals of type-3b CBCs. The immunostaining results are consistent with the findings of previous electrophysiological recordings that T-type Ca^{2+} channels are located both in the soma and at the axon terminal of bipolar cells (Pan, 2000; Pan et al., 2001). The subcellular localization pattern could be important for understanding the potential physiological functions of T-type Ca^{2+} channels in bipolar cells. In general, Ca^{2+} channels in dendrites can facilitate synaptic signal integration while Ca^{2+} channels at the axon terminals can facilitate or directly trigger transmitter release (Huguenard 1996; Dunlap et al., 1995).

Our electrophysiological results suggest that the T-type Ca^{2+} currents in the $Ca_v3.2$-expressing type-3b CBCs are likely to be mainly composed of $Ca_v3.2$ Ca^{2+} channels because a marked reduction of the T-type Ca^{2+} current was observed in a subgroup of type-3 CBCs in $Ca_v3.2$ KO mice. The results appear to also suggest that the type-3b T-type Ca^{2+} current is formed by other T-type Ca^{2+} channel α1 subunits in addition to $Ca_v3.2$ because the T-type Ca^{2+} current was not totally absent in Type-3 CBCs from KO mice. However, it should be noted that the Cav3.2 KO mouse line used in this study is a global knockout model (Chen et al., 2003). Therefore, it is possible that the remaining T-type Ca^{2+} current observed in type-3b CBCs from Cav3.2 KO mice is the result of functional compensation by other T-type Ca^{2+} channel α1 subunits due to knockout of Cav3.2. This question can be addressed when conditional knockout animal models become available. Nevertheless, our results suggest that the T-type Ca^{2+} currents in the PKAβII-positive type-3b CBCs are at least mainly composed of $Ca_v3.2$ channel subunits.

The finding in this study of the expression of $Ca_v3.2$ Ca^{2+} channels in a specific bipolar cell type supports previous reports of the heterogeneous properties of T-type Ca^{2+} currents among bipolar cells and a differential expression of three T-type Ca^{2+} channel subunits among different retinal bipolar cells (Pan, 2000; Hu et al., 2009). What would be the possible functional implications of the expression of $Ca_v3.2$ Ca^{2+} channels in a specific bipolar cell type in particular and the heterogeneous expression of different T-type Ca^{2+} channels in different bipolar cells in general? In the mammalian retina, there is one type of rod bipolar cells and more than 10 types of CBCs (Euler and Wässle, 1995; Ghosh et al., 2004; Pignatelli and Strettoi, 2004; Mataruga et al., 2007; Fyk-Kolodziej and Pourcho,

2007; Cui and Pan, 2008). Bipolar cells are commonly believed to play an important role in segregating visual information into multiple parallel information pathways in the retina (Wässle, 2004). T-type Ca^{2+} currents were previously shown to be essential for the initiation of spontaneous activity in bipolar cells and to contribute to regenerative spike-like potentials (Ma and Pan, 2003; Hu et al., 2009). Increasing evidence suggests that regenerative potentials or spiking activity may play a role in bipolar cell processing (Dreosti et al., 2011; Saszik and DeVries, 2012). Furthermore, T-type Ca^{2+} channels at the axon terminal of bipolar cells are capable of triggering transmitter release (Pan et al., 2001; Singer and Diamond, 2003). Because T-type Ca^{2+} currents with different α1 subunits exhibit different activation and inactivation kinetics and could be subjected to distinct regulation by endogenous substances (Todorovic et al., 2001; Chemin et al., 2006; Traboulsie et al., 2007; Hildebrand et al., 2007; Nelson et al., 2007; Perez-Reyes, 2010), a differential expression of multiple T-type Ca^{2+} channels in different bipolar cell types could result in diversified signal processing and thus contribute to parallel visual information processing in the retina. In particular, the fast inactivation of T-type Ca^{2+} currents could be used for transmitting high frequency visual signals, possibly related to processing temporal visual information, such as motion and directional selectivity. In this regard, it is interesting to note that the axon terminals of type-3 CBCs show overlap with OFF cholinergic band. Therefore, it is possible that the Cav3.2-positive cells form synaptic contact with cholinergic amacrine cells, the cells underlying the generation of direction selectivity in the retina (Lee and Zhou, 2006; Demb, 2007), and/or direction- selective retinal ganglion cells. Thus, further studies are needed to investigate whether the Cav3.2 Ca^{2+} channels in specific and the T-type Ca^{2+} currents in general can contribute to temporal information processing in the retina.

Acknowledgments

This work was supported by NIH Grants EY17130 to Z.-H.P and core Grant EY04068 to Department of Anatomy and Cell Biology at Wayne State University, and in part by an unrestricted Grant from Research to Prevent Blindness to the Department of Ophthalmology, Wayne State University School of Medicine.

Abbreviations

KO	knock out
CBC	cone bipolar cell
HEK	human embryonic kidney
PB	phosphate buffer
OPL	outer plexiform layer
IPL	inner plexiform layer
HCN4	hyperpolarization-activated and cyclic nucleotide-gated channel 4

Reference

Cain SM, Snutch TP. Contributions of T-type calcium channel isoforms to neuronal firing. Channels. 2010; 4:475–82. [PubMed: 21139420]

Carbone E, Giancippoli A, Marcantoni A, Guido D, Carabelli V. A new role for T-type channels in fast “low-threshold” exocytosis. Cell Calcium. 2006; 40:147–54. [PubMed: 16759700]

Chemin J, Monteil A, Perez-Reyes E, Bourinet E, Nargeot J, Lory P. Specific contribution of human T-type calcium channel isotypes [α(1G), α(1H) and α(1I)] to neuronal excitability. J Physiol. 2002; 540:3–14. [PubMed: 11927664]

Chemin J, Traboulsie A, Lory P. Molecular pathways underlying the modulation of T-type calcium channels by neurotransmitters and hormones. Cell Calcium. 2006; 40:121–134. [PubMed: 16797700]

Chen CC, Lamping KG, Nuno DW, Barresi R, Prouty SJ, Lavoie JL, Cribbs LL, England SK, Sigmund CD, Weiss RM, Williamson RA, Hill JA, Campbell KP. Abnormal coronary function in mice deficient in alpha1H T-type Ca^{2+} channels. Science. 2003; 302:1416–8. [PubMed: 14631046]

Cui J, Pan Z-H. Two types of cone bipolar cells express voltage-gated Na^{+} channels in the rat retina. Visual Neurosci. 2008; 25:635–645.

Cui J, Ma Y-P, Lipton SA, Pan Z-H. Glycine receptors and glycinergic synaptic input at the axon terminals of mammalian retinal rod bipolar cells. J Physiol. 2003; 553:895–909. 2003. [PubMed: 14514876]

de la Villa P, Vaquero CF, Kaneko A. Two types of calcium currents of the mouse bipolar cells recorded in the retinal slice preparation. Eur J Neurosci. 1998; 10:317–323. [PubMed: 9753140]

Demb JB. Cellular mechanisms for direction selectivity in the retina. Neuron. 2007; 55:179–186. [PubMed: 17640521]

Dreosti E, Esposti F, Baden T, Lagnado L. In vivo evidence that retinal bipolar cells generate spikes modulated by light. Nat Neurosci. 2011; 14:951–952. [PubMed: 21706020]

Dunlap K, Luebke JI, Turner TJ. Exocytotic Ca^{2+} channels in mammalian central neurons. Trends Neurosci. 1995; 18:89–98. [PubMed: 7537420]

Euler T, Wässle H. Immunocytochemical identification of cone bipolar cells in the rat retina. J Comp Neurol. 1995; 361:461–478. [PubMed: 8550893]

Fyk-Kolodziej B, Pourcho RG. Differential distribution of hyperpolarization-activated and cyclic nucleotide-gated channels in cone bipolar cells of the rat retina. J Comp Neurol. 2007; 501:891–903. [PubMed: 17311321]

Ghosh KK, Bujan S, Haverkamp S, Feigenspan A, Wässle H. Types of bipolar cells in the mouse retina. J Comp Neurol. 2004; 469:70–82. [PubMed: 14689473]

Haverkamp S, Wässle H. Immunocytochemical analysis of the mouse retina. J Comp Neurol. 2000; 424:1–23. [PubMed: 10888735]

Hildebrand ME, David LS, Hamid J, Mulatz K, Garcia E, Zamponi GW, Snutch TP. Selective inhibition of Cav3.3 T-type calcium channels by Galphaq/11-coupled muscarinic acetylcholine receptors. J Biol Chem. 2007; 282:21043–21055. [PubMed: 17535809]

Hu C, Bi A, Pan Z-H. Differential expression of three T-type calcium channels in retinal bipolar cells in rat. Visual Neurosci. 2009; 26:177–187.

Huguenard JR. Low-threshold calcium currents in central nervous system neurons. Annu Rev Physiol. 1996; 58:329–348. [PubMed: 8815798]

Kaneko A, Pinto LH, Tachibana M. Transient calcium current of retinal bipolar cells of the mouse. J Physiol. 1989; 410:613–629. [PubMed: 2552084]

Lee S, Zhou ZJ. The synaptic mechanism of direction selectivity in distal processes of starburst amacrine cells. Neuron. 2006; 51:787–799. [PubMed: 16982423]

Ma Y-P, Pan Z-H. Spontaneous regenerative activity in mammalian retinal bipolar cells: roles of multiple subtypes of voltage-dependent Ca^{2+} channels. Visual Neurosci. 2003; 20:131–139. 2003.

Mataruga A, Kremmer E, Müller F. Type 3a and type 3b OFF cone bipolar cells provide for the alternative rod pathway in the mouse retina. J Comp Neurol. 2007; 502:1123–1137. [PubMed: 17447251]

McRory JE, Santi CM, Hamming KS, Mezeyova J, Sutton KG, Baillie DL, Stea A, Snutch TP. Molecular and functional characterization of a family of rat brain T-type calcium channels. J Bio Chem. 2001; 276:3999–4011. [PubMed: 11073957]

Molineux ML, McRory JE, McKay BE, Hamid J, Mehaffey WH, Rehak R, Snutch TP, Zamponi GW, Turner RW. Specific T-type calcium channel isoforms are associated with distinct burst phenotypes in deep cerebellar nuclear neurons. Proc Natl Acad Sci USA. 2006; 103:5555–5560. [PubMed: 16567615]

Nelson MT, Joksovic PM, Su P, Kang H-W, Deusen AV, Baumgart JP, David LS, Snutch TP, Barrett PQ, Lee J-H, Zorumski CF, Perez-Reyes E, Todorovic MS. Molecular mechanisms of subtype-

specific inhibition of neuronal T-type calcium channels by ascorbate. J Neurosci. 2007; 27:12577–12583. [PubMed: 18003836]

Pan Z-H. Differential expression of high- and two types of low-voltage-activated calcium currents in rod and cone bipolar cells of the rat retina. J Neurophysiol. 2000; 83:513–527. [PubMed: 10634892]

Pan ZH, Hu HJ, Perring P, Andrade R. T-type Ca2+ channels mediate neurotransmitter release in retinal bipolar cells. Neuron. 2001; 32:89–98. [PubMed: 11604141]

Perez-Reyes E. Molecular physiology of low-voltage-activated T-type calcium channels. Physi Rev. 2003; 83:117–161.

Perez-Reyes E. Molecular characterization of T-type calcium channels. Cell Calcium. 2006; 40:89–96. [PubMed: 16759699]

Perez-Reyes EG. Protein-mediated inhibition of Cav3.2 T-type channels revisited. Mol Pharmacol. 2010; 77:136–138. [PubMed: 19903827]

Pignatelli V, Strettoi E. Bipolar cells of the mouse retina: a gene gun, morphological study. J Comp Neurol. 2004; 476:254–266. [PubMed: 15269969]

Protti DA, Llano I. Calcium currents and calcium signaling in rod bipolar cells of rat retinal slice. J Neurosci. 1998; 18:3715–3724. [PubMed: 9570802]

Saszik S, DeVries SH. A mammalian retinal bipolar cell uses both graded changes in membrane voltage and all-or-nothing Na+ spikes to encode light. J Neurosci. 2012; 32:297–307. [PubMed: 22219291]

Lee, Sherwin C.; Hayashida, Yuki; Ishida, Andrew T. Availability of Low-Threshold $Ca2^{+}$ Current in Retinal Ganglion Cells. J Neurophysiol. 2003; 90:3888–3901. [PubMed: 14665686]

Singer JH, Diamond JS. Sustained Ca2+ entry elicits transient postsynaptic currents at a retinal ribbon synapse. J Neurosci. 2003; 23:10923–10933. [PubMed: 14645488]

Talley EM, Cribbs LL, Lee J-H, Daud A, Perez-Reyes E, Bayliss DA. Differential distribution of three membranes of a gene family encoding low voltage-activated (T-type) calcium channels. J Neurosci. 1999; 15:1895–1911. [PubMed: 10066243]

Todorovic SM, Jevtovic-Todorovic V, Meyenburg A, Mennerick S, Perez-Reyes E, Romano C, Olney JW, Zorumski CF. Redox modulation of T-type calcium channels in rat peripheral nociceptors. Neuron. 2001; 31:75–85. [PubMed: 11498052]

Traboulsie A, Chemin J, Chevalier M, Quignard JF, Nargeot J, Lory P. Subunit-specific modulation of T-type calcium channels by zinc. J Physiol. 2007; 578:159–171. [PubMed: 17082234]

Wässle H. Parallel processing in the mammalian retina. Nat Rev Neurosci. 2004; 5:747–757. [PubMed: 15378035]

Highlights

$Ca_v3.2$ Ca^{2+} channel antibody was confirmed in HEK cell expression system and in $Ca_v3.2$ KO mice.

Immunostaining shows the expression of $Ca_v3.2$ Ca^{2+} channels in a subgroup of type-3 bipolar cells.

The immunostaining results were confirmed by patch-clamp recordings.

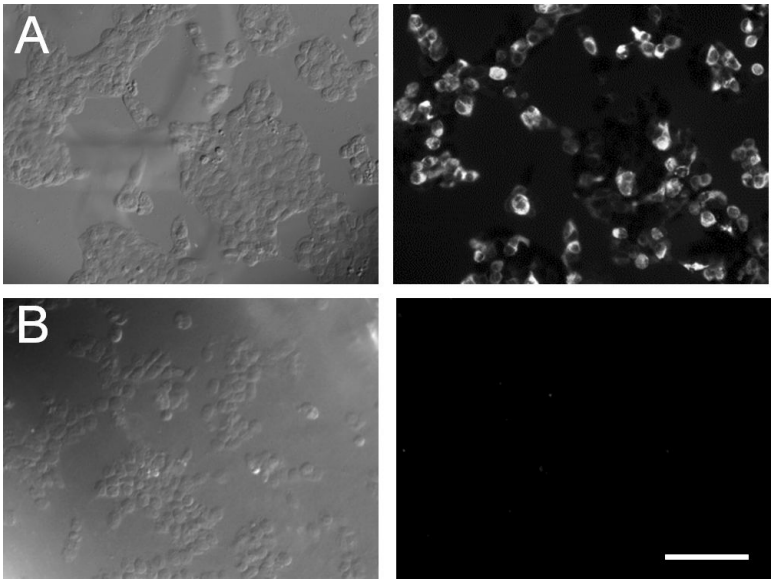

Figure 1. Confirmation of the specificity of a $Ca_v3.2$ Ca^{2+} channel antibody in an HEK cell expression system

HEK cells transfected with (A) or without (B) $Ca_v3.2$ Ca^{2+} channel subunits and labeled with the goat anti-$Ca_v3.2$ antibody conjugated to Alexa 595. (A) Positive immunolabeling of $Ca_v3.2$ was observed in the $Ca_v3.2$ Ca^{2+} channel subunit-transfected HEK cells. (B) No immnunolabeling of $Ca_v3.2$ was observed in the untransfected HEK cells. The left and right panel show the transmission and fluorescence images, respectively. Scale bar: 100 μm.

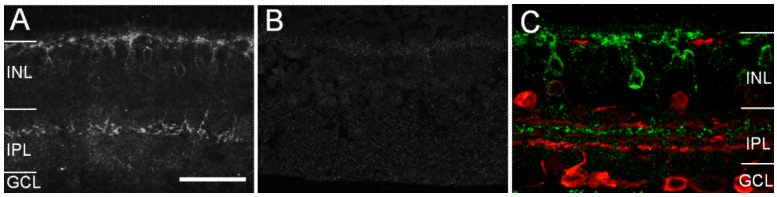

Figure 2. Immunolabeling of $Ca_V3.2$ in retinal vertical sections of wild-type and $Ca_V3.2$ KO mice

(A) The fluorescence signal of immunolabeling of $Ca_V3.2$ in the retinal vertical section of wild-type mouse. The $Ca_V3.2$ immunolabeled cells are bipolar cells with their dendrites located in the outer plexiform layer and axon terminals narrowly stratified in the inner plexiform layer. (B) No immunoactivity to $Ca_V3.2$ was detected in the retinas of $Ca_V3.2$ KO mice. (C) The colabeling of $Ca_V3.2$ (green) and calretinin (red) in the retinal vertical section of wild-type mouse. The axon terminals of $Ca_V3.2$-immunopositive bipolar cells were located between the two distal calretinin bands. Scale bar: 50 μm.

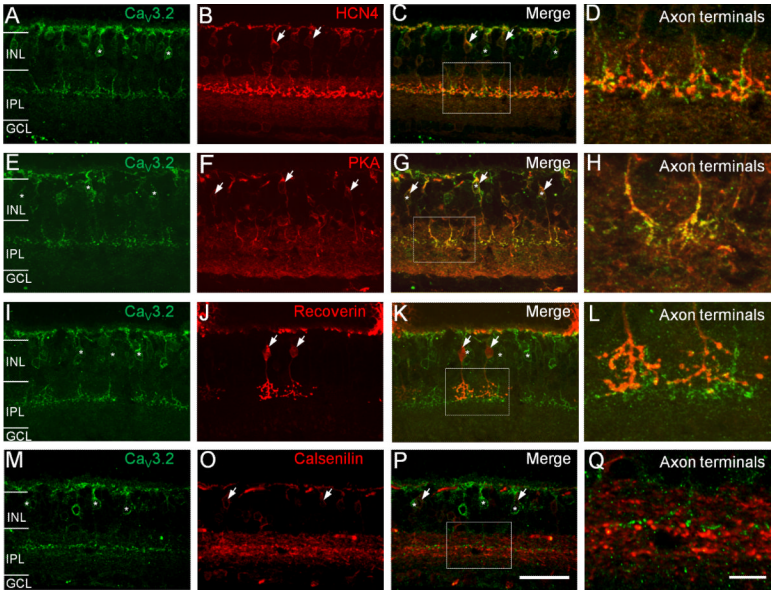

Figure 3. Double-labeling analysis of $Ca_V3.2$-positive bipolar cells in wild-type mouse retinas

(A–D) $Ca_V3.2$-positive bipolar cells (A, green, asterisks) do not show labeling by an antibody against HCN4 (B, red, arrows) as indicated by the lack of colabeling of $Ca_V3.2$ and HCN4 in somata and axon terminals (D). To obtain a better view of the axon terminals, the rectangular region in (C) is shown in (D) at higher magnification. (E–H) $Ca_V3.2$-positive bipolar cells (E, green, asterisks) were also labeled by an antibody against PKAIIβ (F, red, arrows), as demonstrated by the co-labeling of $Ca_V3.2$ and PKAIIβ both in the soma and axon terminals (G and H). $Ca_V3.2$-positive bipolar cells did not show colabeling with recoverin (I–L) and calsenilin (M–Q). Scale bar: 50 μm for the images in the first three columns and 10 μm for the images in the last column.

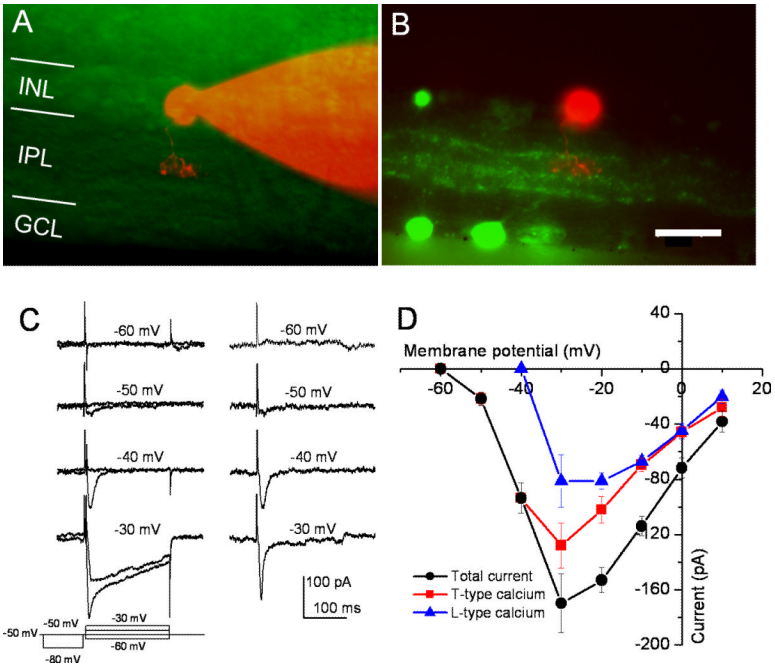

Figure 4. Voltage-gated Ca^{2+} currents of the type-3 cone bipolar cells in wild-type mice

(A) A recorded type-3 cone bipolar cell in a retinal slice preparation filled with the fluorescent dye Alexa 568 through the recording electrode. (B) The retinal slice was immunolabeled with an antibody against calretinin (green). (C) A representative recording of Ca^{2+} currents from type-3 cone bipolar cells (left panel). To separate T- and L-type Ca^{2+} currents, prepulses of −80 and −50 mV (1 s) were applied before a brief (5 ms) depolarization to −50 mV followed by 200 ms test pulses ranging from −60 to −30 mV. The subtracted currents (right panel) represent T-type currents. (D) The I–V relationships of the T-, L-, and the total Ca^{2+} currents (mean ± SE; n = 6).

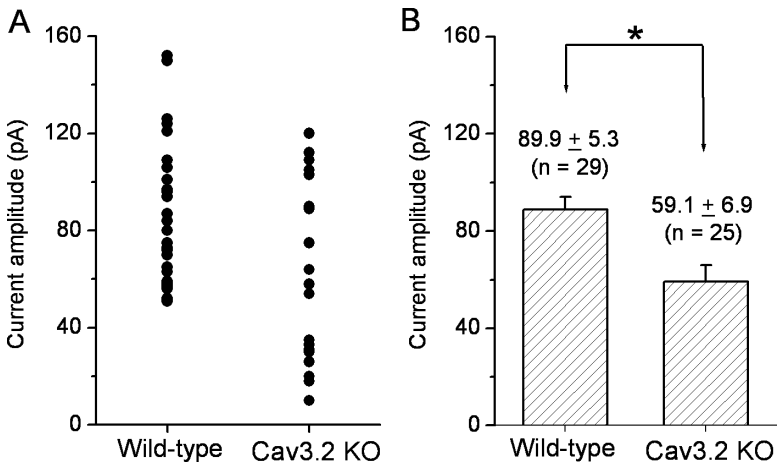

Figure 5. Comparison of T-type currents in type-3 cone bipolar cells between wild-type and $Ca_v3.2$ KO mice

The T-type Ca^{2+} currents were evoked by depolarizing the membrane potential to −40 mV from the holding potential of −80 mV. (A) The current amplitude distribution for all recorded cells from wild-type and $Ca_v3.2$ KO mice. (B) The average values of the T-type Ca^{2+} currents for wild-type and $Ca_v3.2$ KO mice. These two values are significantly different (mean ± SE; $P < 0.005$).